*Proc. Natl. Acad. Sci. USA*
Vol. 91, pp. 11646–11650, November 1994
Neurobiology

# Connectional topography in the zebrafish olfactory system: Random positions but regular spacing of sensory neurons projecting to an individual glomerulus

(*Danio rerio*/axon tracing/neuronal specificity/1,1′-dioctadecyl-3,3,3′,3′-tetramethylindocarbocyanine perchlorate/chloromethylaminocoumarin)

HERWIG BAIER*†, STEFAN ROTTER‡, AND SIGRUN KORSCHING*

Departments of *Physical Biology and ‡Molecular Biology, Max-Planck-Institut für Entwicklungsbiologie, P.O. Box 2109, D-72011 Tübingen, Germany

*Communicated by Christiane Nüsslein-Volhard, June 8, 1994 (received for review March 17, 1994)*

**ABSTRACT** **It is unknown how neuronal connections are specified in the olfactory system. To define rules of connectivity in this system, we investigated whether the projection of sensory neurons from the olfactory epithelium to the olfactory bulb is topographically ordered. By backtracing with 1,1′-dioctadecyl-3,3,3′,3′-tetramethylindocarbocyanine perchlorate (DiI), we find that neurons projecting into a single identified glomerulus are widely dispersed over the olfactory epithelium. Their positions in the sensory surface do not predict their glomerulus specificity and are probably random. A statistical analysis reveals that neurons connected to the same glomerulus are spaced at distances of several cell diameters from each other. The convergence of projections to one point in the target area from neurons that are widely and evenly distributed in the sensory surface constitutes an unusual type of connectional topography that contrasts with the precise topological (neighborhood-preserving) maps found in other sensory systems. It may maximize the probability to detect odorants that activate a single glomerular unit.**

Specific neuronal connections are a prerequisite for the enormous sensitivity and discriminative capacity of the olfactory system. In the visual, somatosensory, auditory, and other sensory systems, neighborhood relationships of peripheral neurons in the sensory surface are faithfully rebuilt by the projection to the central target area (1). In contrast, the primary olfactory projection does not generate a strictly topological map of the olfactory epithelium onto the olfactory bulb (2–6). Indeed, such a map would make sense only if stimulation of neighboring sensory cells carried information about similarity of the stimuli. This seems not to be the case for the primary process of olfaction. However, the degree of anatomical order varies among species: while the projection is seemingly diffuse in the trout (2), it is comparatively ordered in rodents mapping longitudinal stripes of the epithelium onto regions of the bulb (3, 4). These variations cannot be attributed to differences in olfactory ability, since in fish (as in rodents) the sense of smell is highly developed and important for behavior (7).

The olfactory bulb contains numerous neuropil conglomerates, called glomeruli, as primary relay stations for incoming sensory information. Olfactory sensory neurons located in the olfactory epithelium send one axon each into one glomerulus. Several studies have suggested that glomeruli serve as functional modules (8) by responding selectively to specific odorants (9–11). It is conceivable, although not yet shown, that sensory neurons expressing a particular odorant receptor molecule (12) converge into single glomeruli. In any case, glomeruli represent the obvious targets for investigating the connectivity of the olfactory system, but they have not been experimentally accessible in many cases because of their small size and large number in animals commonly studied.

In adult zebrafish (*Danio rerio*), the glomerular array is highly stereotyped (13). Twenty-two glomeruli (about one fourth of the population) can be reproducibly found in all animals, permitting us to systematically study the connections of individually identified glomeruli and compare the patterns for one homologous glomerulus in many animals. We chose the ventroposterior glomerulus (vpG) for most of our backlabeling experiments. It is easily accessible for microinjection with 1,1′-dioctadecyl-3,3,3′,3′,-tetramethylindocarbocyanine perchlorate (DiI) (14) in aldehyde-fixed tissue. Also, it is large and isolated enough to restrict the dye label to this particular glomerulus. Sensory neurons in the olfactory epithelium that project into the ventroposterior glomerulus (vpG) become subsequently labeled by diffusion of DiI along their axons. The resulting backlabeling patterns were analyzed by several criteria for regularities in cell distributions.

## MATERIALS AND METHODS

**Anterograde Prelabeling of Glomeruli with 7-Amino-4-chloromethylcoumarin (CMAC).** To visualize the entire pattern of glomeruli, the blue fluorescent dye CMAC (Molecular Probes; A-2110; 0.5 mg/10 μl in dimethylformamide diluted 1:20 in water) is injected into both nasal cavities of a living, anaesthetized adult fish (see ref. 13). After an overnight tracing period, the fish is killed. Its olfactory system is dissected *en bloc* and fixed (4% paraformaldehyde in 0.1 M phosphate buffer). The dye anterogradely labels sensory terminals in the bulb (Fig. 1 *a* and *b*). The staining can be viewed under the fluorescence microscope with a band-pass 365-nm excitation filter, a 395-nm dichroic mirror, and a long-pass 397-nm emission filter.

**Retrograde Tracing from a Single Glomerulus.** A pulled-out glass micropipette with a broken-off tip is backfilled with a solution of DiI (5 mg/ml of dimethylformamide; Molecular Probes, D-282). The micropipette is connected by thick-walled tubing to an air-pressure injection unit (pneumatic drug ejection system; NPI Instruments, Tamm, F.R.G.) controlled by a stimulus generator (World Precision Instruments). The injection is controlled under a ×10 objective on a fixed-stage fluorescence microscope (Zeiss) by using an exchangeable fluorescence filter set for viewing both CMAC and DiI. For DiI, a standard rhodamine filter set is used.

The publication costs of this article were defrayed in part by page charge payment. This article must therefore be hereby marked "*advertisement*" in accordance with 18 U.S.C. §1734 solely to indicate this fact.

Abbreviations: DiI, 1,1′-dioctadecyl-3,3,3′,3′-tetramethylindocarbocyanine perchlorate; CMAC, 7-amino-4-chloromethylcoumarin; vpG, ventroposterior glomerulus.

†To whom reprint requests should be addressed.

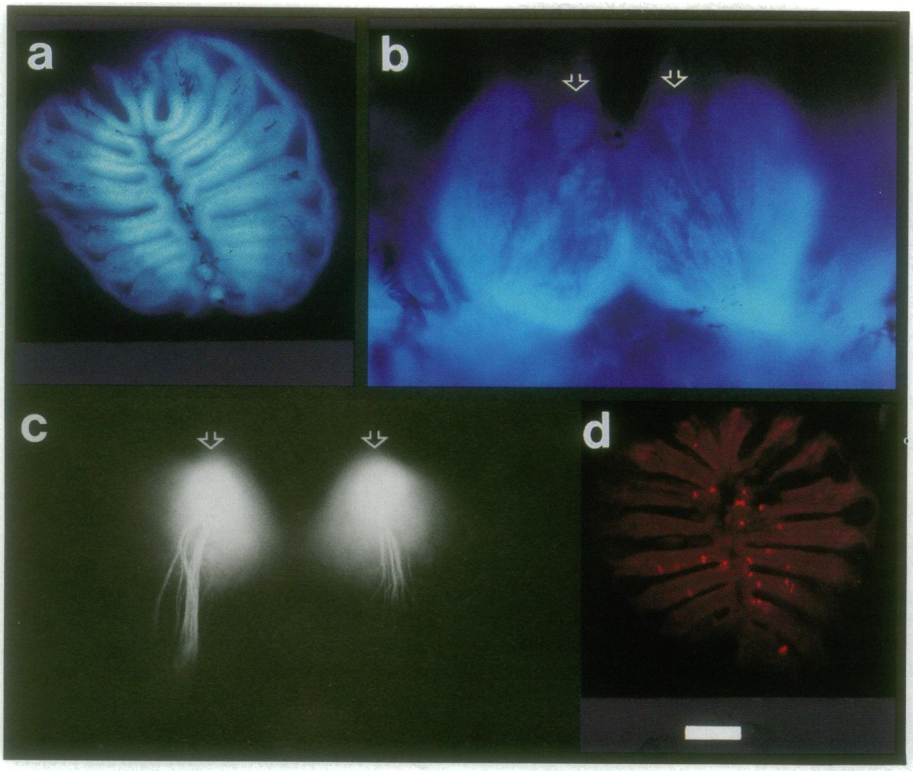


FIG. 1. Backtracing of olfactory sensory neurons projecting into a single glomerulus. (*a*) Olfactory epithelium, 15 hr after CMAC injection. Cells in the central part of the organ (the sensory area) are predominantly stained. (*b*) Pair of olfactory bulbs, immediately before DiI injection. CMAC-labeled glomeruli are easily recognized. The vpGs are indicated by arrows. (*c*) Pair of olfactory bulbs, one week after DiI injection into the vpGs (arrows). Although the dye label has broadened by diffusion, labeled axons emerge only from the initial injection site. (*d*) Olfactory epithelium, 2 weeks after DiI injection into the vpG, displaying individual retrogradely labeled neurons. For *a–d*, posterior is to the top, and anterior is bottom. (Bar = 200 μm.)

While CMAC fluorescence is viewed, the micropipette is positioned into the vpG with the help of a hydraulic micromanipulator (Narishige, Tokyo) mounted on a multidimensional manipulator (Leitz). A small volume (several hundred picoliters) of dye is expelled by air-pressure pulses (300 kPa; 20 ms). The subsequent tracing lasts about 2 weeks, when the tissue is incubated in 0.5% paraformaldehyde (pH 9.8) at 40°C.

By the end of the tracing period, the lateral spread of DiI around the injection site is judged by microscopic inspection. Only those experiments in which the dye-labeled sensory axons emanated exclusively from the vpG were included in this study (Fig. 1*c*). Epithelia containing labeled cells are embedded at a consistent orientation in 7.5% gelatin (in phosphate-buffered saline) and postfixed for 24 hr (4% paraformaldehyde in 0.1 M phosphate buffer). Five or six 100-μm sections are obtained from one epithelium with a vibratome. Generally, only the middle three sections contain labeled cells. The outline of the midmost section of each olfactory epithelium was drawn, and the positions of DiI-labeled cells were charted (see Fig. 2).

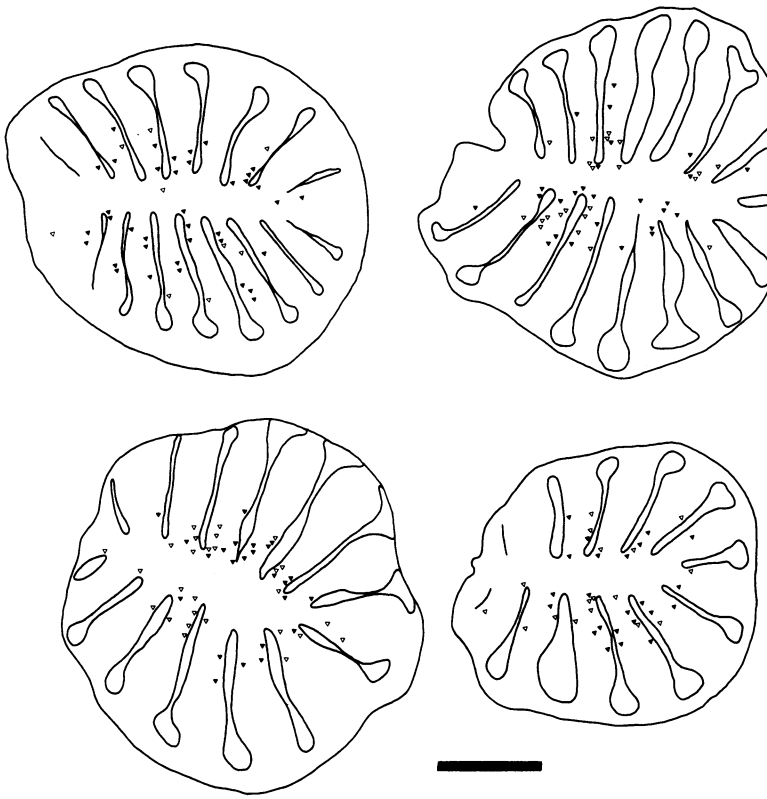

FIG. 2. Sensory neurons projecting to a single glomerulus are scattered over the olfactory epithelium. Four examples of backlabeling patterns. Filled triangles (▼) represent cells found in the middle section. This section was drawn and superimposed by cells found in adjacent sections (▽), with their horizontal positions being approximately conserved. (*Upper Left*) A left-sided epithelium, where medial is top. For all other epithelia, medial is bottom. In all cases, anterior is to the right. (Bar = 200 μm.)

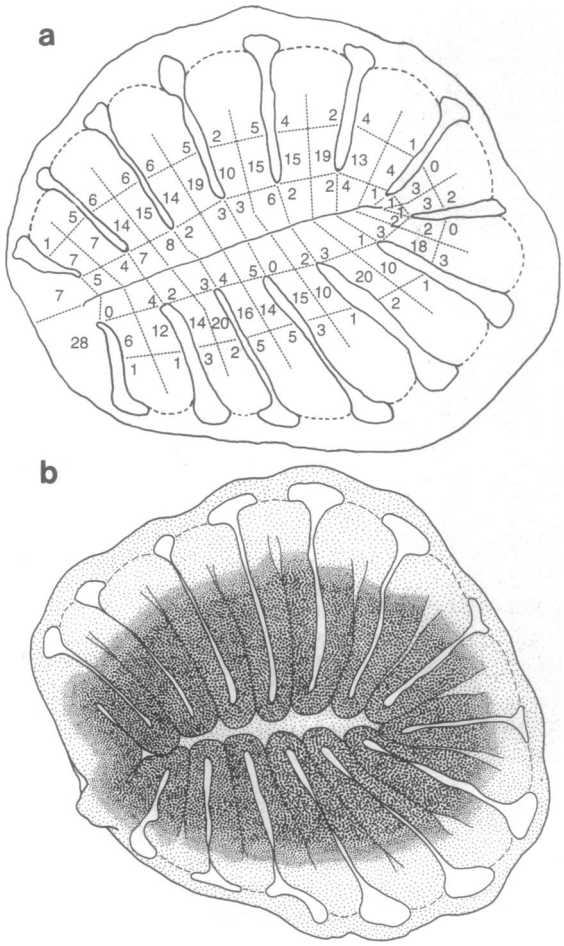


FIG. 3. Distribution of labeled cells within the sensory area of the olfactory organ. (*a*) Prototype epithelium, displaying the cumulative number of labeled cells found within 80 subregions (data from 24 experiments). (*b*) The sensory area (dark) of the epithelium extends over the central two-thirds of the lamellae. Non-sensory epithelium (bright gray) is present at the median raphe and on the peripheral parts of the lamellae. This drawing was obtained from an experiment in which a large amount of DiI was injected into the olfactory nerve at its junction with the bulb. For *a* and *b*, anterior is left, and medial is top.

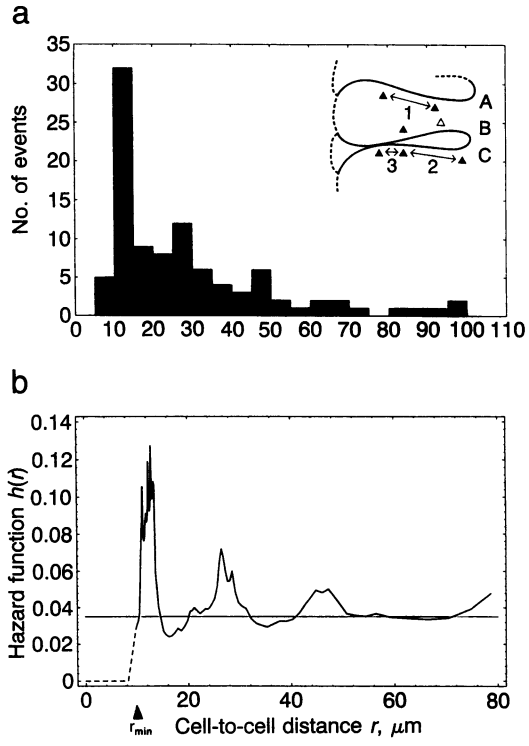


FIG. 4. Nearest-neighbor distances ($n$ = 98) for neurons projecting to a single glomerulus. (*a*) Histogram. A one-dimensional Poisson point process would yield an exponentially decreasing function. In contradiction to this hypothesis, small distances are underrepresented; the histogram peaks at 10–15 μm. (*Inset*) Three half-lamellae from top to bottom (A, B, and C) of an olfactory epithelium with several labeled cells (symbolized as in Fig. 2) visualize how the cell-to-cell distances (three values in this case) were obtained (see *Materials and Methods*). The position of the letters A, B, and C also indicates the approximate position of the median raphe. (*b*) Hazard function $h(r)$ (see *Materials and Methods*). For a Poisson process, the data should approximate the straight line shown, which equals the inverse of the mean distance ($\bar{r}$ = 28.6 μm). They do so for large but not for small distances. The smallest distance found is indicated by an arrow ($r_{min}$ = 8.2 μm). Unit of the hazard function is $\mu m^{-1}$.

The data from 24 successful backtracing experiments were pooled by determining the cumulative number of cells found in 80 subregions of the epithelium. Numbers were plotted onto a prototype epithelium to obtain Fig. 3*a*. Epithelia may vary in the number of lamellae (11, 13 or 15) depending on the age of the fish. This would impede comparisons between experiments. However, during growth of the animal, pairs of lamellae appear in a posterior-to-anterior sequence (15, 16). Thus, homologous lamellae can be allocated safely, except for the two ontogenetically youngest (the anterior-most) in old fish (with 15 lamellae). Labeled cells on those were summarized on the anterior parts of the prototype epithelium without further subdivision.

**Frequency Distribution of Cell-to-Cell Distances.** Distances between nearest neighbors were measured on digitized drawings of all vpG-backtracing patterns by using image-processing software (NIH IMAGE 1.52) on a Macintosh computer. Only the midmost sections of the epithelia were evaluated. Every half-lamella was analyzed separately (as a continuous sheet of sensory epithelium) in a predefined sequence, avoiding double counts. This procedure is illustrated schematically by Fig. 4*a Inset*. Measured distances correspond to projections of the actual distances onto the plane of section. The null hypothesis for subsequent statistical testing is "complete randomness" for the distribution of cells in the (two-dimensional) epithelium—i.e., the result of a Poisson process with spatially homogeneous rate parameter (measured in cells per unit area). This is the case where the cells take random positions irrespective of their distances from other cells. Projecting a Poisson distribution in a plane onto a line again results in a Poisson distribution. Therefore, the null hypothesis carries over to the projected (now one-dimensional) data to which the test is actually applied. Projections of point processes, however, will generally produce relatively more short distances on a line than there are in the plane. Our results still show a significant lack of short distances whatsoever, leading us to reject the null hypothesis (see *Results*). In addition, we performed simulations to ascertain that the characteristic shape of the histogram does not simply reflect projection artifacts (data not shown).

A more direct interpretation of the deviations from our null hypothesis can be achieved by means of the so-called hazard function (17). The hazard function $h(r)$ is derived from the empirical distribution of cell-to-cell distances. It was determined numerically from the unbinned data by using routines written in MATHEMATICA on a workstation. Starting with the empirical survivor function $S(r)$ = no. (distances > $r$)/no. (all distances), the hazard function is obtained by differentiating their negative logarithm: $h(r) = -\frac{d}{dr} \log S(r)$. In our case, this was done by linear regression over every 10 contiguous data points of the empirical survivor function. Since there were no

distances between 0 and $r_{min}$ = 8.2 μm, the empirical hazard function is necessarily 0 in this range. For the Poisson case, one would find the hazard-function to be constant: $h(r) = 1/\bar{r}$ (with $\bar{r}$ being the mean distance).

## RESULTS

In total, we performed 98 injections of DiI into the vpGs of 49 animals. In 24 preparations, >1 backlabeled neuron could be observed in the corresponding olfactory epithelia by the end of the tracing period. The number of these cells was on average 21, with a maximum of 79. Rough estimates of the total number of mature sensory neurons in one epithelium (25,000) and the fraction of these projecting to the vpG (*ca.* 1%) suggest that at most one-third (on average 10%) of all neurons connected to the vpG become labeled by our method. These figures are in accord with a number of DiI tracing studies describing that the dye labels a random subset of axons.

Neurons backlabeled from the vpG were found scattered within the entire sensory area of the epithelium (Fig. 1*d*). We did not observe a deviation from this pattern in any of our 24 successful experiments (Fig. 2 shows 4 examples). Labeled cells were never found to be regionally clustered. Since in each tracing experiment a variable subset of neurons projecting to the vpG was labeled, it could not be precluded that a more subtle topographical ordering was overlooked by separate evaluations. Pooling the data from all individuals would enhance a tendency of labeled cells toward accumulating in certain parts of the epithelium. Since lamellae can be homologized from fish to fish by their positions in the organ, each epithelium could be consistently divided into 80 subregions (see *Materials and Methods*). The total number of cells found within corresponding subregions was plotted onto a prototype epithelium (Fig. 3*a*). The pooled data confirm that labeled neurons are widely distributed over all lamellae.

The area where labeled neurons are located exactly matches the sensory area of the olfactory organ, as was shown by a massive DiI injection of the bulb at the olfactory nerve's entry point. This leads to backlabeling of many thousands of neurons in the olfactory epithelium (Fig. 3*b*). Olfactory sensory neurons in the zebrafish form a continuous sheet lining the walls of the lamellae within the central two-thirds of their lengths, a pattern that is typical for cyprinid fish (15). Cell bodies of zebrafish olfactory neurons extend over 2–3 μm in the tangential direction of the epithelium and are in many cases directly apposed. We estimate the mean distance between two neighboring neurons to be 3–4 μm, well in accord with earlier studies in other teleosts (15, 16).

In the vpG-backtracing experiments, we find that labeled neurons do not reside at reproducible positions in different animals (as judged by the distance from the median raphe) but are scattered in an unpredictable manner along the lamella (data not shown). Although a deterministic pattern cannot be disproven, it seems most likely that the spatial coordinates of these neurons within the sensory area are random.

The absence of region-to-region mapping could be generalized to the entire olfactory projection by 34 backtracings from other glomerular positions. We performed injections into the ventrocentral part of the olfactory bulb ($n$ = 7), the ventromedial ($n$ = 6), the ventroanterior ($n$ = 3), the ventrolateral ($n$ = 1), the dorsal ($n$ = 2), and the ventroposterior part ($n$ = 15). In some cases, injections were confined to a single glomerulus, as with the vpG. The backtracing patterns obtained did not appear different for different injection sites, while the number of labeled cells correlated with the size of the injection.

We reasoned that, even in the absence of global order, local ordering principles could govern the positions of backlabeled neurons relative to each other. Alternatively, cell positions could be independent from each other—i.e., generated in the manner of a Poisson point process (17). To decide on this, we measured lateral distances between neighboring cells in the data set from the vpG backtracings. Because of the complex geometry of the sensory epithelium, distances can be determined reliably only within one-half lamella and within that in one dimension of the plane of section. We therefore obtained the distance data as described in *Materials and Methods* and as illustrated in the Fig. 4*a Inset*. In case of a one-dimensional Poisson process, one would expect a frequency distribution that starts with a high number at small distances and declines exponentially for larger distances. The empirical data are shown in the histogram of Fig. 4*a*. It is obvious that small distances are absent—i.e., less frequent than expected from the Poisson hypothesis. The absence of close neighbors cannot be explained trivially by the cell-body diameter, which is only 2–3 μm (see above).

To obtain a more sensitive indicator for deviations from a Poisson point process, we calculated the so-called hazard function (see *Materials and Methods*) of our data. Fig. 4*b* shows the empirical results as well as the theoretical function predicted by a Poisson process. In the theoretical case, the hazard function has a constant value equal to the inverse of the mean distance. The empirical function apparently deviates from the theoretical function in several respects (for a test of significance, see below) as follows: (*i*) as already indicated by the histogram (Fig. 4*a*), small distances are absent; (*ii*) distances around 13 μm occur at a much higher than average rate; and (*iii*) the function declines rapidly at 16–20 μm and rises again with a second peak at about 27 μm. To indicate the significance of these features, we performed a maximum-likelihood fit of the empirical survivor function to an exponential distribution. We tested the goodness-of-fit by using appropriate $\chi^2$ statistics and found that the difference between the empirical and the fitted function is statistically significant ($\alpha < 0.001$). To determine significance of individual structural components of the distribution, the test was applied separately to truncated data sets in which only distances above a certain threshold were used. By systematically varying this threshold, we find that for distances > 15 μm, the Poisson hypothesis cannot be rejected ($\alpha > 0.2$). In conclusion, this analysis demonstrates that the relative lack of small distances (<11 μm) and the overrepresentation of distances around 13 μm (first peak) are significant, whereas the other peaks and depressions are not. Nevertheless, the latter could reflect trends in the data, which we could not resolve with our method.

From the statistical analysis, it is clear that neurons connected to the vpG keep a minimum distance from each other. The hazard function further suggests that neighbors that are absent in the vicinity of a particular cell occur at more distant positions instead. In statistical terms, this phenomenon argues for "repulsion" as the spacing mechanism, rather than "elimination." An elimination process would yield a curve starting and saturating similarly, but without overshooting in the intermediate range. While it is clear that a statistical description cannot predict a biological mechanism, it narrows the range of possibilities.

## DISCUSSION

Our study demonstrates that sensory neurons with a single glomerulus as common target are evenly distributed within the olfactory epithelium. The absolute positions of these neurons within the sensory surface seem to play no role in determining their target specificity. This contrasts strikingly with many other neuronal systems, where position of a neuron in an embryonic field is a key determinant of its later connectivity. For example, in the visual system, retinal

ganglion cells are specified by their position in the retinal field to project to a defined point in the midbrain (18). As a consequence of this specification, the visual field is mapped topologically onto the corresponding brain area. Our data show that the olfactory epithelium lacks this type of global positional information. This finding is consistent with an earlier report on the olfactory projection to glomerular regions in trout (2) and extends its conclusions to single glomeruli in zebrafish. This "anti-topological" principle does not strictly apply to other vertebrates, like rodents (3, 4). However, regional correspondence between the olfactory epithelium and the bulb in these species is coarse and may reflect developmental events unrelated to target specification (4). A new and unpredicted finding in zebrafish is that neurons with the same target are not dispersed randomly over the sensory surface but are evenly spaced. It will be interesting to see whether this observation can be generalized to other vertebrates.

Several cell-biological mechanisms are conceivable to cause the spacing of equally specified cells. Any model has to take into account the fact that there are about 80 glomeruli in the zebrafish (in addition to uncompartmentalized glomerular plexus), all of which serve as potential target sites for outgrowing sensory axons. In other vertebrate species, glomeruli are much more numerous (e.g., several thousands in rodents), making the problem of target specificity still more complex.

A brute-force programming mechanism, at one extreme, would tell every single neuron from its birth which glomerulus to choose as a target (i.e., to determine its "specificity type"). Our study predicts that the programming (if it exists) would not rely on the absolute position of a neuron, as for the retinal ganglion cells, because neighboring neurons in one epithelium are specified in completely different directions, as are neurons at a particular position in different epithelia. Rather, the observed distribution could occur as a result of a non-random stem-cell division scheme. Stem cells of sensory neurons are situated in a basal layer just underneath the sensory neuron sheet. From the patterns observed, we have reason to believe that individual stem cells can produce many, if not all, specificity types of sensory neurons. A successive generation of different types, with all of the already existing types being excluded, would give rise to a heterogeneous clone consisting of cells of one type each. Since clones are likely to form spatial clusters separated from neighboring clones, the distance between cells of the same type would be determined by the size of a single clone. In this model, regular spacing is a secondary effect of the clonal exclusion at the stem cell level. No further mechanisms are necessary.

An alternative group of models involves cross-talk between postmitotic but partly uncommitted sensory neurons. One plausible mechanism uses lateral inhibition: neurons with a particular specificity may biochemically suppress parallel differentiation of neighboring neurons. An equivalent mechanism has been demonstrated in the development of the photoreceptor mosaic in the *Drosophila* eye (19). In our case, the statistical analysis of cell-to-cell distances predicts that the biochemical signal would be short-ranging (a few cell diameters). Also, it would not simply remove the inhibited cell but instead would induce its displacement or, more likely, generation of another cell of this type at a more distant position. In a straightforward but uneconomical version, the diversity of biochemical signals necessary would be as large as the number of glomeruli. It could be reduced if an additional mechanism (e.g., detection of coincident activity) were taken into account. In an alternative scenario, repulsion could take place between axons at the level of the olfactory nerve. It has been reported for several vertebrate species including the trout (2) that axons abruptly lose their peripheral neighborhood relationships when entering the olfactory bulb, suggesting some form of axon–axon repulsion at this site.

To decide on which mechanism is true, it is essential to know whether sensory neurons are predetermined to select a specific glomerulus before their axons reach the glomeruli. It is possible that these neurons initially project randomly into the glomerular layer and then receive a target-specific signal from the glomerulus that directs their differentiation (e.g., odorant receptor expression). Such retrograde instruction by the target would provide for functional specificity while permitting a stochastic projection mode. In any case, we show here that the specification of olfactory neurons is not completely without topographic order. Thus, a one-way mechanism relying solely on retrograde instruction of randomly projecting neurons does not seem to be true.

Many investigators assume that glomeruli serve as functional units by integrating information about odors reaching the sensory epithelium. In a simple case, sensory neurons carrying the same odor receptor molecules would converge into single glomeruli (8–11, 20). Consistent with this notion, *in situ* hybridizations in the catfish (20) have revealed that cells expressing a particular odorant receptor molecule are distributed over the olfactory epithelium, in a manner very similar to what we find for cells backlabeled from single glomeruli. It will be necessary to combine the two methods to find out whether receptor molecule expression and target specificity are indeed correlated. In terms of biological function, an even distribution of sensory neurons connected to one functional unit (i.e., a glomerulus) seems to be favorable; by this a single functional unit may sample over a larger area and maximize the probability to detect an odorant present in low concentration (under certain conditions; see ref. 21) or contained in a microheterogeneous odor plume.

We thank F. Weth, W. Nadler, A. Gierer, and B. Hellwig for helpful discussions and F. Bonhoeffer for generous support and advice. C. Gitter kindly took care of the zebrafish colony and K.-H. Nill contributed parts of the drawings. H.B. is supported by a fellowship of the Boehringer Ingelheim Fonds.

1. Udin, S. B. & Fawcett, J. W. (1989) *Annu. Rev. Neurosci.* **11,** 289–327.
2. Riddle, D. R. & Oakley, B. (1991) *J. Neurosci.* **11,** 3752–3762.
3. Jastreboff, P. J., Pedersen, P. E., Greer, C. A., Stewart, W. B., Kauer, J. S., Benson, T. E. & Shepherd, G. M. (1984) *Proc. Natl. Acad. Sci. USA* **81,** 5250–5254.
4. Astic, L., Saucier, D. & Holley, A. (1987) *Brain Res.* **424,** 144–152.
5. Mackay-Sim, A. & Nathan, M. H. (1984) *Anat. Embryol.* **170,** 93–97.
6. Duncan, H. J., Nickell, W. T., Shipley, M. T. & Gesteland, R. C. (1990) *J. Comp. Neurol.* **299,** 299–311.
7. Little, E. E. (1983) in *Fish Neurobiology*, eds. Northcutt, R. G. & Davis, R. E. (Univ. Michigan Press, Ann Arbor, MI), Vol. 1, pp. 351–375.
8. Shepherd, G. M. (1992) *Nature (London)* **358,** 457–458.
9. Lancet, D., Greer, C. A., Kauer, J. S. & Shepherd, G. M. (1982) *Proc. Natl. Acad. Sci. USA* **79,** 670–674.
10. Buonviso, N. & Chaput, M. A. (1990) *J. Neurophysiol.* **63,** 447–454.
11. Imamura, K., Mataga, N. & Mori, K. (1992) *J. Neurophysiol.* **68,** 1986–2002.
12. Buck, L. & Axel, R. (1991) *Cell* **65,** 175–187.
13. Baier, H. & Korsching, S. (1994) *J. Neurosci.* **14,** 219–230.
14. Godement, P., Vanselow, J., Thanos, S. & Bonhoeffer, F. (1987) *Development (Cambridge, U.K.)* **101,** 697–713.
15. Yamamoto, M. (1982) in *Chemoreception in Fishes*, ed. Hara, T. J. (Elsevier, Amsterdam), pp. 39–59.
16. Holl, A. (1965) *Z. Morphol. Ökol. Tiere* **54,** 707–782.
17. Cox, D. R. & Lewis, P. A. W. (1966) *The Statistical Analysis of Series of Events* (Methuen, London).
18. Fraser, S. E. (1992) *Curr. Opin. Neurobiol.* **2,** 83–87.
19. Greenwald, I. & Rubin, G. M. (1992) *Cell* **68,** 271–281.
20. Ngai, J., Chess, A., Dowling, M. M., Necles, N., Macagno, E. R. & Axel, R. (1993) *Cell* **72,** 667–680.
21. Berg, H. C. & Purcell, E. M. (1977) *Biophys. J.* **20,** 193–219.